SAR Analysis of New Dual Targeting Fluoroquinolones. Implications of the Benzenesulfonyl Group

Marcelo J. Nieto[a], Adriana B. Pierini[b], Nidhi Singh[c], Christopher R. McCurdy[c,d], Ruben H. Manzo[e], María R. Mazzieri[e]*

[a]*Department of Pharmaceutical Sciences, School of Pharmacy, Southern Illinois University Edwardsville, Edwardsville, IL, 62026, USA*

[b]*Departamento de Química Orgánica, Facultad de Ciencias Químicas, Universidad Nacional de Córdoba, Ciudad Universitaria, 5000 Córdoba, Argentina*

[c]*Department of Medicinal Chemistry, Research Institute in Pharmaceutical Sciences, School of Pharmacy, The University of Mississippi, University, MS, 38677, USA*

[d]*Research Institute in Pharmaceutical Sciences, School of Pharmacy, The University of Mississippi, University, MS, 38677, USA*

[e]*Departamento de Farmacia, Departamento de Química Orgánica, Facultad de Ciencias Químicas, Universidad Nacional de Córdoba, Ciudad Universitaria, 5000 Córdoba, Argentina*

Abstract: When a benzenesulfonyl moiety (BS) was bound to the N-piperazinyl ring of antibacterial fluoroquinolones (AMFQs) norfloxacin (NOR) or ciprofloxacin (CIP), the resulting benzenesulfonyl-fluoroquinolone (BSFQs) analogs showed an improved *in vitro* activity against Gram-positive strains. A bioisosterical replacement of the sulfonyl group for a carbonyl group led to the benzenecarboxamide-fluoroquinolones (BCFQs) that showed a similar trend in the antibacterial activity and spectrum. The BSFQs and BCFQs are considered members of the "dual targeting" fluoroquinolones, targeting both DNA gyrase and topoisomerase IV. To disclose the real contribution of the BS/BC moiety in anti-staphylococcal activity, a 3D-QSAR analysis that included calculation of theoretical molecular descriptors and pharmacophore generation was performed. Previous and present QSAR results have confirmed the positive influence on activity of small electron donating *p*-substituent on the BS or BC moiety. The generated phamacophore model showed that both phenyl and SO_2/CO groups are involved in the interaction with receptor. We postulate that the enhanced potency of BSFQs against *Staphylococcus aureus* compared to CIP and NOR could be caused by the presence of the BS moiety that resulted in enhanced binding to DNA gyrase of Sa. Additionally, their greater ability to enter bacterial cells by diffusion and a reduced susceptibility to FQ-specific efflux pumps could also make a contribution.

Keywords: Benzenesulfonyl group, conformational analysis, fluoroquinolones, pharmacophore, QSAR.

INTRODUCTION

The design of antibacterial fluoroquinolones (AMFQs)[1] having "dual targeting" mechanism of action is a very interesting research objective owing to the increasing emergence of multidrug-resistant pathogens. These AMFQs, acting by inhibiting both DNA gyrase and topoisomerase IV, would need two target mutations to develop resistance [1, 2]. According to SAR studies, substituent at the 7-position has a great impact on modulating potency, spectrum of activity, resistance, intracellular accumulation, biopharmaceutics, and pharmacokinetic properties [3]. Previous studies have shown that the substituent at the 7-position interact with the enzymes by electrostatic forces [3, 4]. Thus, the optimization of the structure of AMFQs towards improving the dual targeting mechanism, would necessary implicate modifications of the substituent at the 7-position.

Benzenesulfonylamido-fluoroquinolones (BSFQs, **1-10**, Table **1**) are a new class of AMFQs reported previously by Manzo *et al.* [5, 6]. Some of these BSFQs exhibited higher in vitro activity against *Staphylococcus aureus* ATCC 29213 [7-9] (Sa) and also against Gram-positive clinical strains compared to ciprofloxacin (CIP) and norfloxacin (NOR), their parent compounds [10]. The new analogs have, as a unique structural feature, *p*-substituted benzenesulfonamide groups (BS) bound to the free nitrogen of the piperazine. The

*Address correspondence to this author at the Departamento de Farmacia, Departamento de Química Orgánica, Facultad de Ciencias Químicas, Universidad Nacional de Córdoba, Ciudad Universitaria, 5000 Córdoba, Argentina; Tel: +54-351-4334127; Fax: +54-351-4334163;
E-mails: mrmazzie@fcq.unc.edu.ar; maria_mazzieri@yahoo.com.ar

[1]BS, benzenesulfonyl moiety; BC, benzenecarboxamide moiety; FQ, fluoroquinolone ; AMFQs, antibacterial fluoroquinolones; NOR, norfloxacin; CIP, ciprofloxacin; BSFQs, benzenesulfonyl-fluoroquinolone; BCFQs, benzenecarboxamide-fluoroquinolones; Sa, *Staphylococcus aureus* ATCC 29213; ax-ax, axial-axial; ax-eq, axial-equatorial; eq-ax, equatorial-axial; eq-eq, and equatorial-equatorial; HBA, hydrogen bond acceptor; HBD, hydrogen bond donor; HYD, hydrophobicity; RA, ring aromatic; PI, positive ionizable; MIC_M, Molar Minimum Inhibitory Concentration; Q_{Xn}, Mulliken charges (X = C, N, or O); $OU_{eq/ax}$, bond order.

new BSFQs, initially designed as hybrid drugs, exert their biological action through a quinolone-like mechanism, which account for the improved anti-staphylococcus activity, with no contribution of the sulfa mechanism of action [7-9]. Furthermore, Fisher *et al.* [1, 11] studied the action of compound **1b** finding that it is a dual target agent in Sa and *Streptococcus pneumoniae* unlike CIP, its precursor, whose target preference is the topoisomerase IV [1, 8, 11]. Therefore, the BS substituent at the 7-position and its proper stereoelectronic characteristics could explain the distinctive biological activity of the BSFQs [8, 9] Indeed, we have previously reported the QSAR studies of *p*-substituted-benzenesulfonamide derivatives of NOR and CIP, which revealed that the electronic distribution and the steric effects of the BS strongly influence the activity, while the lipophilic properties would have no contribution [8, 9]. Finally, a replacement of the sulfonyl group for a carbonyl group led to the benzenecarboxamido-fluoroquinolones (BCFQs, **11-13**), which are considered true bioisosters of BSFQs, albeit with lower activity [12].

The aim of this work is to disclose the real contribution of the BS or BC moiety to the mechanism of action of AMFQs by performing molecular modeling experiments comprised of 3D-QSAR and pharmacophore generation. First, a conformational analysis was performed in order to assess the geometry of these compounds. Second, an integrated approach combining molecular modeling energy refinements with quantum chemical QSAR was investigated. Finally, an automated pharmacophore hypothesis generation was carried out. The information collected provides a potential explanation for the structural requirements of these dual-targeting BSFQs.

METHODS

Computational Resources

Molecular modeling was performed on a Silicon Graphics Octane2 R12000dual processor workstation running on Irix 64 (SGI, 1600 amphitheater Parkway, Mountain view, CA 94043). Pharmacophore modeling was performed using Catalyst 4.8 [13]. The starting geometries were generated by optimization of structures built with the molecular modeling package MOLDEN [14] by means of molecular orbital AM1[15] calculation using AMPAC program [16]. The conformational analysis, the electronic studies, and the calculation of numerical descriptors were performed with WIN-MOPAC program [17] and the QSAR studies with Stat v4.0 [18].

Conformational Analysis

The molecular conformation of the BSFQs and BCFQs is determined by five principal torsional angles as shown in Fig. (**1**): (1) the dihedral angle φ1 defines the ethyl or cyclopropyl relative position with respect to the quinolone plane; (2) the dihedral angle φ2 defines the carboxyl relative position with respect to the carbonyl group of the quinolone ring; (3) the dihedral angle φ3 defines the orientation of the quinolone ring (FQ) with respect to the piperazinyl ring; (4) the dihedral angle φ4 defines the BS/BC moiety relative position with respect to the piperazinyl ring (or FQ ring); and (5) the

dihedral angle φ5 defines the orientation of the benzene ring with respect to the sulfonyl/carbonyl group (or the piperazinyl ring).
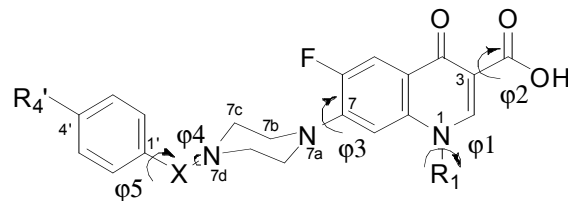
1, BSFQs: X = SO$_2$; R$_1$ = C$_2$H$_5$, *c*C$_3$H$_5$
BCFQs: X = CO; R$_1$ = C$_2$H$_5$, *c*C$_3$H$_5$

Fig. (1). General structure of the BSFQs and BCFQs showing the torsional angles that define their conformation.

In the present study, the following aspects have been considered: (i) the spatial disposition of the substituents in the piperazinyl ring, axial-axial (ax-ax), axial-equatorial (ax-eq), equatorial-axial (eq-xx), and equatorial-equatorial (eq-eq); (ii) the neutral form for all the structures, and (iii) only chair conformation for the piperazine ring.

In order to find the minimum energy conformations of the BSFQs and BCFQs, a complete conformational analysis was carried out, in steps of 15º for both equatorial and axial conformers. The lower-energy conformers of the unsubstituted structures (**6a**, **6b**, **12a**, and **12b**) resulting from the general conformational analysis were used as the stable structures to minimize the other members of the series of BSFQs (and BCFQs). Each molecule was minimized using AM1 [15] force field. These energy-minimized structures were used as starting points for the calculation of the molecular descriptors.

Generation of Pharmacophores

A pharmacophore model in *Catalyst* is generally referred to as a ''hypothesis'', which consists of a collection of features (e.g., hydrogen bond acceptor, HBA; hydrogen bond donor, HBD; hydrophobicity, HYD; ring aromatic, RA; positive ionizable, PI) necessary for the biological activity of the ligands oriented in 3D space [19]. In order to generate a pharmacophore, all molecules (both training and test sets, Table **1**) were built and minimized within *Catalyst*. Conformation models for all molecules were generated using the quasi-exhaustive *Catalyst*/*ConFirm* module within the software, using the ''best quality'' conformational search option. A maximum of 250 conformations were generated using CHARMm force field parameters [20] and a constraint of 20 kcal/mol energy thresholds above the global energy minimum. Catalyst selects conformers using the Poling algorithm [21], which penalizes any newly generated conformer if it is too close to an already formed conformer in the set. This method ensures maximum coverage in conformational space. All other parameters were set to the default settings. The uncertainty value represents a ratio range of uncertainty in the activity value based on the expected statistical straggling of biological data collection. The *Catalyst*/*HypoGen* module can only generate a maximum of five features for hypothesis. The best model was selected on the basis of a high correlation coefficient (r), lowest total cost, and rms values.

Cost function analysis. The quality of the generated hypotheses was evaluated by considering the cost functions (represented in bits unit) relative to the null and fixed hypothesis calculated by the *Catalyst*/*HypoGen* module during hypothesis generation. The total cost of any hypothesis should be toward the value of the fixed cost to represent any useful model. It has been suggested in the *Catalyst* that the differences between the cost of the generated hypothesis and the null hypothesis cost should be as large as possible; a value of 40–60 bits difference may indicate that most probably it has a 75–90% chance of representing a true correlation in the data set used. Furthermore, the configuration cost for any generated hypothesis should be less than or equal to 17 (corresponds to 217 pharmacophore models). Any value higher than 17 may indicate that the correlation from any generated pharmacophore is most likely due to chance since *Catalyst* cannot consider more than these models in the optimization phase and so the rest are left out of the process. The rmsd represent the quality of the correlation between the estimated and the actual activity data.

Cross-validation test. To further assess the statistical significance of the pharmacophore hypotheses generated from the training set molecules a validation procedure, based on Fischer's randomization test [22] was applied. The point of this test is to establish the strong correlation between chemical structures and biological activity. The activity values of the training set molecules are scrambled randomly using the *CatScramble* technique, available in the *Catalyst*/*HypoGen* module, and new spreadsheets are created. The number of spreadsheets generated depends on the level of statistical significance one wants to achieve. For a 95% confidence level, 19 spreadsheets are created. For 98% and 99% confidence levels, 49 and 99 spreadsheets, respectively, are created. In our validation test, we selected the 95% confidence level, and 19 spreadsheets were created by the *CatScramble* command.
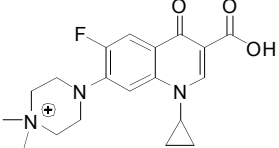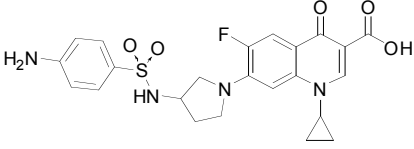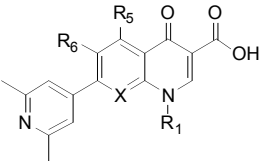
RESULTS

Structures and Biological data

Table **1** shows the structures of all the molecules used in the present study (training and test set) and antibacterial activity (IC$_{50}$, µM) calculated as the negative logarithm of the Molar Minimum Inhibitory Concentration (MIC$_M$) against Sa [5, 7-9, 12]. Activity against other microorganisms and clinical strains have been already published [5, 7-9, 12].

Table 1. Structures of the Fluoroquinolones Used in the Present Study and their Antimicrobial Activity Against *Staphylococcus aureus* ATCC 29213
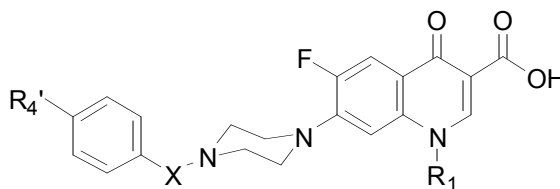
ID	X	R1	R4´	IC$_{50}$ (µM)[a]
1a	SO$_2$	-C$_2$H$_5$	NH$_2$	6.58
1b	SO$_2$	*c*-C$_3$H$_5$	NH$_2$	7.21
2a	SO$_2$	-C$_2$H$_5$	NHCOCH$_3$	5.71
2b	SO$_2$	*c*-C$_3$H$_5$	NHCOCH$_3$	6.02
3a	SO$_2$	-C$_2$H$_5$	N(CH$_3$)COCH$_3$	5.42
3b	SO$_2$	*c*-C$_3$H$_5$	N(CH$_3$)COCH$_3$	5.74
4a	SO$_2$	-C$_2$H$_5$	NHCH$_3$	6.59
4b	SO$_2$	*c*-C$_3$H$_5$	NHCH$_3$	7.22
5a	SO$_2$	-C$_2$H$_5$	N(CH$_3$)$_2$	5.70
5b	SO$_2$	*c*-C$_3$H$_5$	N(CH$_3$)$_2$	6.31
6a	SO$_2$	-C$_2$H$_5$	H	6.57
6b	SO$_2$	*c*-C$_3$H$_5$	H	6.90
7a	SO$_2$	-C$_2$H$_5$	CH$_3$	5.67
7b	SO$_2$	*c*-C$_3$H$_5$	CH$_3$	6.29
8a	SO$_2$	-C$_2$H$_5$	OCH$_3$	5.99
8b	SO$_2$	*c*-C$_3$H$_5$	OCH$_3$	n.d.

Table 1. contd….

ID	X	R1	R4′	IC_{50} (µM)[a]
9a	SO_2	$-C_2H_5$	Cl	5.09
9b	SO_2	c-C_3H_5	Cl	n.d.
10a	SO_2	$-C_2H_5$	NO_2	6.61
10b	SO_2	c-C_3H_5	NO_2	7.24
11a	CO	$-C_2H_5$	NO_2	5.64
11b	CO	c-C_3H_5	NO_2	5.95
12a	CO	$-C_2H_5$	H	5.63
12b	CO	c-C_3H_5	H	6.24
13a	CO	$-C_2H_5$	NH_2	5.36
13b	CO	c-C_3H_5	NH_2	5.68
Norfloxacin				5.80
Ciprofloxacin				6.12
Pefloxacin				5.95
Enoxacin				5.51
Levofloxacin				6.03
Sarafloxacin				6.51
Gatifloxacin				5.49
Me-Pefloxacin				4.34
14				6.59

	R1	R5	R6	X	IC_{50} (µM)
15[23]	c-C_3H_5	F	F	CF	7.68
16	Et	H	F	CH	7.05
17	t-But	H	F	CH	7.09
18	p-C6H4F	H	F	CH	6.51
19	NHCH3	H	F	CH	6.75
20	c-C_3H_5	H	F	CH	7.64
21	c-C_3H_5	H	F	N	7.07
22	c-C_3H_5	H	H	CH	6.74
23	c-C_3H_5	H	F	CF	7.64
24	c-C_3H_5	F	F	CF	7.66

[a]The MIC determination of compounds **1-14** is described in references [5, 7-9], and 12, and [b] Reference [23] describes the experimental determination of the MIC of compounds **15-24**.
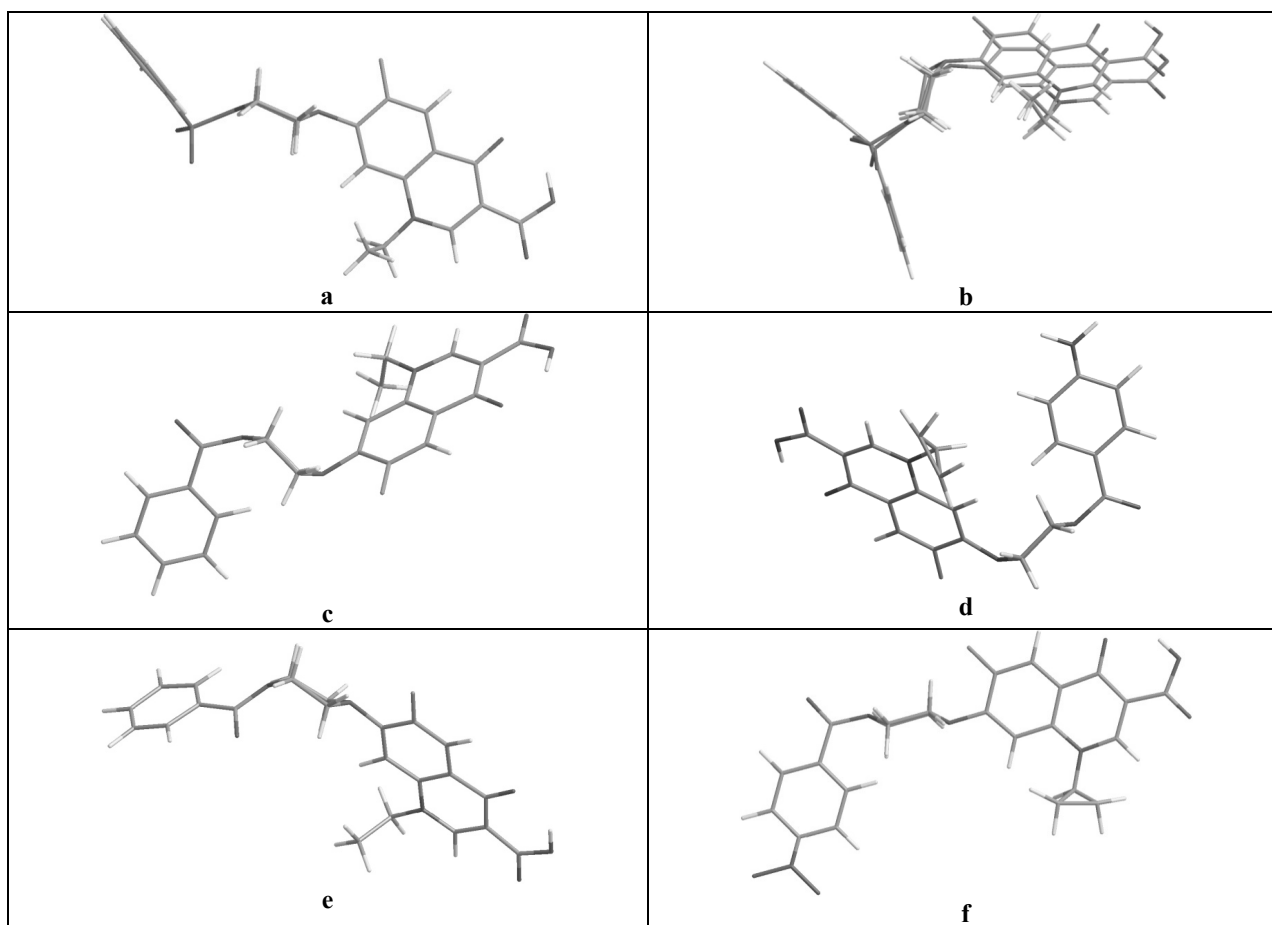
Fig. (2). View of the lower energy conformers for BSFQs and BCFQs. **a**) BSFQ when the FQ group is eq; **b**) Overlay of the two lower energy conformers for the BSFQs when the FQ group is ax; **c**) BCFQ when ax-ax; **d**) BCFQ when ax-eq; **e**) BCFQ when eq-ax; **f**) BCFQ when eq-eq.

Every BSFQs examined was more active against Gram-positive strains than Gram-negative ones [5, 7-9, 12] and showed activity *in vitr*o against Sa, with MICs ranged from 0.03 to 2 μg/mL. The most active compounds were **1**, **4**, **6** and **10** for both series, with *in vitro* activities fourfold higher than their precursors, CIP and NOR. The BCFQs followed the same trend as the BSFQs, showing better activity against Gram-positives than Gram-negatives, with MICs comparable to the prototypes (NOR and CIP) but lower than the BSFQs [9, 12].

Conformational Analysis

In order to evaluate the conformational properties of compounds **1-13**, it was important to find the different combinations of the dihedral angles for each conformer (Fig. **1**). This analysis was performed through a systematic search of the minimum energy conformation by combinations of the rotations of those dihedral angles. The results for the BSFQs series showed that the BS moiety was always in the same spatial disposition (pseudo eq) as determined by the SO$_2$NR$_2$ group, which agrees with previously reported data [24-26]. For the BCFQs, the BC group could adopt two conformations (ax or eq) due to the conjugation of the amide group with the phenyl ring.

All compounds studied showed similar stereochemical features, with the FQ ring being planar and the following

distinctive observations for the dynamical structure description. In both, BSFQs and BCFQs, φ1 determined the conformation of the substituent at the 1-position (Fig. **1**). The results were in agreement with previous findings reported by Ohta *et al.* [27] and Chung *et al.* [28] where the rotation of the ethyl group of NOR led to two possible minima, 100° above and below the FQ plane. Interestingly, for the CIP series, the minima for the cyclopropyl group were 100° above and 40° below the plane of the FQ. The 3-carboxylic group, described by the φ2 angle, can adopt only two possible conformations, 0° and 180°, due to the conjugation of the CO group with the quinolone ring. The ΔE for the conformers was 11.46 kcal/mol, being the more stable the one that could form hydrogen bonding with the 4-keto group. These findings have been also reported by other authors for non-ionized FQs [4, 29]. To study the conformational preferences of the piperazinyl group relative to the FQ system, φ3 angle was selected (Fig. **1**). For the BSFQs, the minima found for both, ax and eq, isomers correspond to a molecular arrangement where the 6-fluoro was distant to the lone-pair electrons at the N$_{7a}$ (Fig. **1**) of the piperazinyl ring and close to the hydrogens of the adjacent carbons (7b and 7`b, Fig. **1**). Moreover, the results showed that the conformation of the BS/BC moiety do not affect the conformation of the FQ. Finally, rotations of φ4 and φ5 resulted in four stable conformers for the BSFQs (Fig. **2a-b**) and eight for the BCFQs (Fig. **2c-f**). Due to the symmetry of the BS moiety of the

Table 2. Delta Energy for the BCFQs Isomers.

	ax-ax				ax-eq				eq-ax				eq-eq		
φ_4	ΔE (kcal/mol)		φ_4		ΔE (kcal/mol)		φ_4		ΔE (kcal/mol)		φ_4		ΔE (kcal/mol)		
	$\varphi_5 = 0$	$\varphi_5 = 180$			$\varphi_5 = 0$	$\varphi_5 = 180$			$\varphi_5 = 0$	$\varphi_5 = 180$			$\varphi_5 = 0$	$\varphi_5 = 180$	
60	0.000	1.054	210		0.175	0.243	210		0.128	0.000	210		0.543	0.475	
300	0.492	0.270	300		0.222	0.000	270		1.732	1.726	300		0.000	0.795	

Table 3. 3D-QSAR Descriptors for BSFQ Series

#	HOMO		LUMO		$Q_{C1'}$		$Q_{C2'}$		$Q_{C3'}$		$Q_{C4'}$	
	ax	eq	ax	eq	ax	eq	ax	eq	ax	eq	ax	eq
1a	-9.058	-9.216	-0.905	-0.899	-0.238	0.161	0.161	0.158	0.158	-0.237	-0.906	-0.972
1b	-9.051	-9.196	-0.904	-0.899	-0.237	0.161	0.161	0.157	0.157	-0.237	-0.891	-0.956
2a	-9.085	-9.189	-0.872	-0.872	-0.190	0.150	0.150	0.151	0.151	-0.220	-0.951	-1.003
2b	-9.077	-9.216	-0.871	-0.868	-0.192	0.149	0.149	0.148	0.148	-0.220	-0.962	-0.979
3a	-9.106	-9.303	-0.859	-0.850	-0.166	0.141	0.141	0.139	0.139	-0.193	-0.956	-1.070
3b	-9.054	-9.228	-0.855	-0.854	-0.194	0.138	0.138	0.138	0.138	-0.202	-0.958	-0.992
4a	-9.051	-9.140	-0.904	-0.899	-0.235	0.161	0.161	0.158	0.158	-0.232	-0.903	-0.968
4b	-9.045	-9.133	-0.903	-0.899	-0.232	0.160	0.160	0.159	0.159	-0.236	-0.887	-0.951
5a	-9.035	-8.963	-0.906	-0.901	-0.234	0.171	0.171	0.168	0.168	-0.234	-0.898	-0.961
5b	-9.030	-8.960	-0.905	-0.901	-0.234	0.170	0.170	0.168	0.168	-0.234	-0.883	-0.944
6a	-9.157	-9.277	-0.826	-0.824	-0.155	-0.064	-0.064	-0.065	-0.065	-0.156	-0.996	-1.041
6b	-9.133	-9.256	-0.826	-0.823	-0.155	-0.064	-0.064	-0.065	-0.065	-0.156	-0.982	-1.024
7a	-9.125	-9.265	-0.837	-0.833	-0.159	0.001	0.001	0.000	0.000	-0.161	-0.971	-1.027
7b	-9.117	-9.244	-0.836	-0.833	-0.160	0.001	0.001	0.000	0.000	-0.159	-0.963	-1.011
8a	-9.116	-9.259	-0.873	-0.870	-0.237	0.147	0.147	0.145	0.145	-0.185	-0.958	-1.021
8b	-9.109	-9.239	-0.873	-0.870	-0.235	0.147	0.147	0.145	0.145	-0.185	-0.943	-1.004
9a	-9.175	-9.306	-0.826	-0.822	-0.152	-0.002	-0.002	-0.002	-0.002	-0.153	-1.214	-1.074
9b	-9.166	-9.280	-0.825	-0.822	-0.152	-0.153	-0.002	-0.002	-0.154	-0.153	-1.211	-1.060
10a	-9.286	-9.400	-0.772	-0.769	-0.097	0.095	-0.072	-0.073	-0.094	0.095	-2.044	-1.905
10b	-9.275	-9.378	-0.771	-0.769	-0.097	0.095	-0.072	-0.073	-0.094	0.095	-2.043	-1.900
Δ	0.256	0.440	0.135	0.132	0.141	0.332	0.243	0.241	0.146	0.332	1.161	0.961

BSFQs there were only two distinguishable conformers, which were defined by the N_{7d} of the piperazine with the phenyl group (of the BS) almost perpendicular to the piperazine ring. The relative conformation of both minima reflected a "butterfly-like" conformation around the piperazine (Fig. **2a-b**), which has also been previously described by Benedetti et al. for sulfonamides [24, 26]. This folded form was defined by a pseudo-eq conformation of the BS group in the energy-minimized structures. It has been demonstrated that the nitrogen of the sulfanilamide group differs in properties according to its structural environment,

but it is generally closer to the sp^2 hybridization [30, 31]. We observed this phenomenon when positioning the BS group ax or eq and agrees with Benedetti *et al.* [26] and Bowen *et al.* [31] for sulfonamides series. As a result, the substituent at N_{7b} (BS group) could only adopt one position in contrast to the N1 substituent (FQ ring) that could be ax (Fig. **2a**) or eq (Fig. **2b**).

The BCFQs showed eight conformers, as defined by the conformation of N_{7a} and N_{7d} along with dihedral angles $\varphi4$ and $\varphi5$ (Fig. **2**). Table **2** summarizes the energy and dihedral angles of BCFQs lower energy conformers.

Table 4. Theoretical Electronic Parameters for the BCFQs Isomers

#	Isomer	HOMO	LUMO	$Q_C{}^1$	$Q_O{}^2$	$Q_{C1'}{}^3$	$Q_{C4'}{}^4$	$Q_N{}^5$	$Q_{C7}{}^6$
11a	ax-ax	-9.0848	-0.9409	3.6548	6.3507	4.1165	4.1104	5.3275	3.9222
	ax-eq	-9.0866	-0.9406	3.6524	6.3523	4.1165	4.1104	5.3293	3.9220
	eq-ax	-9.0901	-0.9172	3.6578	6.3505	4.1169	4.1109	5.3216	3.9103
	eq-eq	-9.0901	-0.9172	3.6578	6.3505	4.1169	4.1109	5.3216	3.9103
12a	ax-ax	-9.2549	-1.6283	3.6636	6.3401	4.0745	4.1152	5.3175	3.9255
	ax-eq	-9.2548	-1.6284	3.6637	6.3401	4.0745	4.1152	5.3175	3.9255
	eq-ax	-9.2431	-1.6198	3.6689	6.3398	4.0758	4.1148	5.3102	3.9146
	eq-eq	-9.2431	-1.6198	3.6689	6.3398	4.0758	4.1148	5.3102	3.9146
13a	ax-ax	-8.9542	-0.8881	3.6488	6.3592	4.1726	3.9051	5.3228	3.9202
	ax-eq	-8.9542	-0.8881	3.6488	6.3592	4.1726	3.9051	5.3228	3.9202
	eq-ax	-8.9754	-0.8611	3.6551	6.3588	4.1738	3.9049	5.3135	3.9094
	eq-eq	-8.9754	-0.8611	3.6551	6.3588	4.1738	3.9049	5.3135	3.9094
11b	ax-ax	-9.0636	-0.9197	3.6559	6.3525	4.1177	4.1090	5.3224	3.9231
	ax-eq	-9.0641	-0.9206	3.6583	6.3457	4.1173	4.1101	5.3202	3.9217
	eq-ax	-9.2556	-1.0193	3.6607	6.3478	4.1166	4.1111	5.3147	3.9665
	eq-eq	-9.2556	-1.0193	3.6608	6.3478	4.1166	4.1111	5.3146	3.9665
12b	ax-ax	-9.2369	-1.6759	3.6657	6.3337	4.0739	4.1158	5.3154	3.9269
	ax-eq	-9.2369	-1.6759	3.6660	6.3337	4.0739	4.1165	5.3154	3.9251
	eq-ax	-9.3803	-1.5182	3.6683	6.3356	4.0732	4.1169	5.3100	3.9700
	eq-eq	-9.3803	-1.5180	3.6683	6.3356	4.0732	4.1169	5.3100	3.9700
13b	ax-ax	-8.9771	-0.8787	3.6516	6.3526	4.1709	3.9085	5.3204	3.9203
	ax-eq	-8.9770	-0.8787	3.6516	6.3524	4.1709	3.9084	5.3203	3.9203
	eq-ax	-8.8946	-0.9671	3.6541	6.3546	4.1694	3.9107	5.3151	3.9655
	eq-eq	-8.8946	-0.9671	3.6541	6.3546	4.1694	3.9107	5.3151	3.9655
Δ		0.4857	0.8148	0.0202	0.0255	0.0445	0.2118	0.0193	0.0562

[1]Mulliken charge on the C (carboxamide group); [2] Mulliken charge on the O (carboxamide group); [3] Mulliken charge on the C1'; [4] Mulliken charge on the C4'; [5] Mulliken charge on the N-7d; [6] Mulliken charge on the C7.

QSAR

Based on previous findings, all the descriptors related to those properties presumably involved in the mechanism of action were examined. The relative importance of over fifty parameters had been compared. The construction of a QSAR model was performed by using empiric, semiempiric and theoretical parameters that describe the molecule or its *p*-substituent on the BS/BC moiety. Herein, we present a QSAR study that includes the previously described 2D descriptors (that describe electronic, steric and lipofilic features) along with the 3D steric and electronic parameters obtained from the theoretical analysis [9, 32]. For the calculation of the theoretical descriptors, the more stable conformation of each form, ax and eq, were chosen. The Mulliken charges of the respective atoms are represented as Q_{Xn}, where

X = C, O or N and n is the number according to Fig. (**1**); and OU_{ax} and OU_{eq} are the bond order for the oxygens in the SO_2 group in the ax and eq form, respectively. Table **3** shows some of the most important and statistically significant theoretical descriptors used in these studies. The data for other parameters, not disclosed here but considered in the present study, are available as supplementary material. The descriptors selected for the 3D-QSAR study were the ones that reflected stereoelectronic changes in the 7d-position.

As for the BSFQs, the BCFQs electronic properties were obtained from the conformers with lower energy for each one of the isomers. Table **4** summarizes their selected electronic parameters. It can be observed that most of them were affected in the same way as in the BSFQs. Also, both sets of isomers (ax-ax and ax-eq; eq-ax and eq-eq) had very similar values for the parameters.

Table 5. QSAR Equations Using Semiempirical Descriptors

$IC_{50}=$	Equation #
$0.58(\pm0.10)I$-$1.02(\pm0.13)B_1$-$1.36(\pm0.14)\sigma_p$+$7.15(\pm0.19)$ n=16, r=0.95, SD=0.20, F(3,12)=46.48, p<0.00001	1 [9]
$-0.43(\pm0.24)I$-$053(\pm0.26)B_1$-$4.12(\pm1.54)LUMO_{ax}$+$10.72(\pm1.61)$ n=16, r=0.77, SD=0.45, F(3,12)=5.67, p<0.01	2
$-0.84(\pm0.24)B_1$+$11.97(\pm2.69)LUMO_{ax}$+$19.42(\pm1.61)$ n=16, r=0.80, SD=0.40, F(2,13)=11.89, p<0.01	3
$0.56(\pm0.23)I$-$0.72(\pm0.28)B_1$+$17.20(\pm6.67)C_{2'ax}$+$6.83(\pm0.43)$ n=16, r=0.80, SD=0.42, F(2,13)=6.95, p<0.01	4
$0.58(\pm0.28)I$-$0.51(\pm0.34)B_1$+$1.06(\pm1.73)C_{4'ax}$+$6.60(\pm0.52)$ n=16, r=0.81, SD=0.41, F(2,13)=7.84, p<0.001	5
$0.63(\pm0.21)I$-$0.82(\pm0.26)B_1$-$85.55(\pm25.41)OU_{ax}{}^{a}$+$59.38(\pm15.68)$ n=16, r=0.80, SD=0.40, F(2,13)=11.89, p<0.01	6
$-0.91(\pm0.30)B_1$-$106.41(\pm31.21)OU_{eq}{}^{a}$+$72.95(\pm19.38)$ n=16, r=0.73, SD=0.46, F(2,13)=7.29, p<0.01	7
$0.51(\pm0.22)I$-$0.75(\pm0.27)B_1$-$107.33(\pm0.14)\sigma QO_{eq}{}^{b}$-$92.97(\pm33.45)$ n=16, r=0.79, SD=0.43, F(2,13)=6.58, p<0.01	8

a) OU_{ax} and OU_{eq} are the bond order for the oxygen in the SO_2 group in the ax and eq form, respectively; b) QO_{eq} is the charge on the O of the SO_2 group in the eq form.

We used multiple linear regressions to construct the QSAR model in which the experimental anti-staphylococcal activity was expressed as a linear combination of the descriptors plus a constant. Statistical terms (correlation coefficient, r, F-test, standard deviation, p-value, etc) were used to evaluate the quality of a model. In order to combine NOR and CIP series an indicator variable was included (for NOR, $I = 0$; for CIP, $I = 1$). Single variable equations were analyzed but no good correlations (r < 0.5) were found. These equations were used as starting point for the stepwise regression analysis (SRA). The electronic parameters were selected as the starting point since they showed higher regression coefficients when compared with the steric and hydrophilic ones. The SRA was performed by exploring multi variable equations that included electronic parameters combined with theoretical empirical and semiempirical lipophilic and/or steric parameters. Over one hundred equations were generated and analyzed; those that showed the best correlations when both series were combined (and excluding the NO_2 analogs which was previously defined as an outlier) are shown in Table **5** [8, 9]. The 2D-QSAR equation that best describe the antibacterial activity includes an electronic parameter (σ_p), a steric parameter (B1) and an indicator variable (I). For the 3D-QSAR several molecular (i.e. HOMO and LUMO) or submolecular (i.e. atom charges and OU) electronic indices obtained from molecular modeling calculations have also shown to be useful describing structure-activity relationships (Table **5**). Equations without an indicator variable were also considered since some of the descriptors (in particular HOMO and LUMO) would discriminate between NOR and CIP, as can be appreciated from equations 3 and 7. Equation 1, included in Table **5** for reference, was the result from previous QSAR studies [9].

From the equations showed in Table **5** some considerations can be drawn:

(1) The *p*-substituent on the BS moiety would contribute to discriminate the activity by influencing the stereoelectronic distribution on the sulfonyl group [8, 9].

(2) None of the equations with statistical significance included a hydrophobic parameter.

(3) All the equations resulted with a better regression coefficient when B1 was used as a steric descriptor.

(4) Equations 6-8 could explain the contribution of the electronic distribution on the SO_2 group, described through the theoretical parameters OU_{ax}, OU_{eq}, and QO_{eq}, on the *in vitro* antibacterial activity and spectrum.

(5) From the complete set it is worth mentioning that the steric and electronic parameters have always the same trend, small electron donor groups would favorably affect the *in vitro* bioactivity of this series of compounds against Sa.

Pharmacophore Studies

For the pharmacophore generation a database of 46 fluoroquinolones was built. The database was comprised by: a) compounds **1-13 (**BSFQs and BCFQs)**, 14** and Me-Pefloxacin (previously described by us) [6, 8, 12] b) seven commercially available fluorqouinolones; and c) ten fluoquinolones published by Reuman et al [23] , selected due to the structural diversity and the MIC methodology. An initial analysis revealed that HBA, HYD, and RA could effectively map all critical chemical/structural features of the training set molecules. During the initial phase of the hypothesis generation, it was observed that only two features, i.e. HBA and

HYD, out of those three mentioned above dominated most of the useful hypotheses generated by the *Catalyst*. Therefore, those two features were used by *Catalyst* to generate 10 pharmacophore hypotheses from the training set, using a default uncertainty value of 3. From those, only 8 were statistically significant; and four of them recognized the same structural features in the pharmacophore (Table **6**).

Table 6. Hypotheses Generated by Catalyst.

Hypothesis	r	RMSD	Cost
1	0.92	0.073	67.79
2	0.89	0.077	67.79
3	0.86	0.081	67.79
4	0.89	0.086	67.80
5	0.81	0.091	67.81
6	0.82	0.092	67.81
7	0.79	0.097	67.81
8	0.71	0.104	67.83

Hypothesis 1 was selected (r=0.92) as the best representation of the pharmacophore. As can be appreciated from (Fig. **3**), the structural features identified by *Catalyst* were HBA (green balls) and HYD (blue balls). More specifically, HBAs are localized on the carboxylic acid and the keto of the quinolone ring, and on the sulfonyl moiety of the BSFQs or the carbonyl group of the BCFQs. On the other hand, HYD are localized on the aromatic rings (FQ and BS) and the substituent on N_1 of the FQ ring.
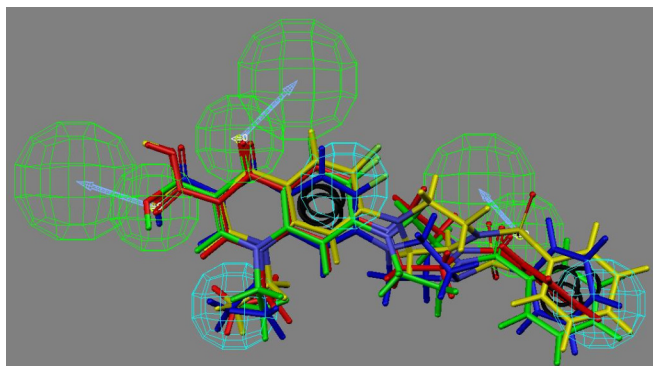

Fig. (3). The structural features identified by *Catalyst*: HBA (H bonding acceptors in green balls) and HYD (Hydrophobicity in blue balls). Superposition of the most representative fluoroquinolones (BSFQ, BCFQ, FQ, NSPQ).

DISCUSSION

Although first designed as hybrids, **1a** and **1b** demonstrated to act primary through quinolone mechanism of action targeting the topoisomerases [7, 11] Moreover, several analogs of the series of BSFQs without the required structural sulfanilyl moiety (*p*-aminophenyl sulfonyl) of the sulfa drugs, displayed similar antibacterial activity than **1a** or **1b** (see **4a-b**; **6a-b** or **10a-b**, Table **1**). This behavior was opposite to other quinolone-containing hybrids via C-7 connec-

tion, such as quinolone-oxazolidinone[33, 34], anilinouracyl-fluoroquinolones [35], rifamycin-quinolones [36], among others [37]. Unlike these hybrids, the BSFQs **1-10**, and their bioisosteric BCFQs **11-13**, displayed an improved activity against Sa. Other AMFQs with bulky substituents on C-7 showed to be more potent against Gram-positive as well [27, 38-46], including dimmers [47, 48]. Since a BS moiety bound to piperazinyl ring is the unique structural change introduced in the series of analogs, the shifting observed in the antibacterial activity should be attributed to it. The bioisosteric replacement of the sulfonyl for a carbonyl group led to six BCFQs that displayed the same behavior. Moreover, the decrease in antibacterial activity of both, BSFQs and BCFQs, against Gram-negative strain should be related to the same structural modification. However, the *in vitro* activity against Sa fluctuated in a wide range of MICs demonstrating that the sole presence of a BS or BC group is not enough to explain the shifting in the antibacterial activity.

The SAR and QSAR results presented herein and in previous publications [8, 9, 12] indicate that stereoelectronic properties of the BS modulated by the *p*-substituent, play a decisive role on the MICs observed in the new series of BSFQs. In fact, substituents in the *p*-position of the phenyl group are essential in discriminating the *in vitro* activity against Sa of the BSFQs, and their bioisosteric BCFQs, being the small electron-donor groups the best ones.

It is known that two factors are responsible for the *in vitro* antibacterial activity of AMFQs:

(i)   The inhibition of the target enzyme (DNA gyrase or topoisomerase IV). The target preference of AMFQs in Gram-positive bacteria is a complex issue: topoisomerase IV appears to be the primary target for CIP, levofloxacin, and trovafloxacin; gyrase may be the primary target for sparfloxacin, nadifloxacin, and WCK-1734; and gatifloxacin, clinafloxacin , gemfloxacin, and moxifloxacin act through either enzyme [2, 44, 45, 49]. Thus, a key to understand quinolone action in Gram-positive bacteria is the observation that the drugs can act preferentially through topoisomerase IV, or DNA gyrase, or both, in a way that is structurally dependent. The enhanced activity of BSFQs against Gram-positive bacteria could be explained as follows: (1) gyrase from Gram-positive bacteria is usually less susceptible to inhibition from AMFQs than gyrase from Gram-negative bacteria; and (2) inhibition of the gyrase is more lethal to the bacteria than the inhibition of topoisomerase IV [45]. Although the structural features responsible for the interaction of AMFQs with the binding sites on gyrase or topoisomerase IV are not yet fully understood, the substituent on C-7 is considered to be the one that directly interacts with either enzyme determining the target preference for AMFQs. Shen *et al.* [4, 50] have demonstrated the importance of the C-7 substituent in drug-enzyme interactions. Furthermore, not only position 7 can tolerate a bulky group, but increasing molecular mass and bulkiness of such substituents increase the potency against Gram-positive bacteria.

(ii) Their accumulation into the bacteria cell. Size and hydrophobicity of the FQ molecules have been also reported to affect accumulation of AMFQs into bacterial cell [51, 52]. Thus, the presence of the BS or BC groups on the piperazine moiety lead to analogs (series BSFQs and BCFQs) with only one ionizable group, while their parent compounds, CIP and NOR, are zwitterionic molecules. This structural feature was considered the most relevant in order to explain the higher uptake of **1b** compared with CIP [7] It has been also reported that bulky substituents on C-7 appear to be the key structural characteristic for avoidance of active drug efflux, preventing the decrease of the intracellular drug concentration. Protection from the bacterial efflux proteins would also diminish the likelihood of bacterial resistance [42].

Previous findings by using 2D-QSAR studies for the congeneric series of BSFQs suggested that the BS group would contribute to discriminate the activity not only by blocking an ionizable center but also, and perhaps more important, by influencing the electronic distribution of the benzene ring. While it was clear that electronic and steric descriptors were the most important ones for predicting potency, it was not evident how these variables were involved in real terms. In this sense, phenyl groups would not influence the quinolone ring system as far as NMR and UV data in solution. These facts would imply that the BS group was not intramolecularly mediating into the quinolone ring system, but could be interacting through intermolecular forces with the enzyme [8]. The results from the 3D-QSAR and pharmacophore generation presented herein suggest that both phenyl and SO_2 moieties of the BS are relevant in molecular target recognition. The aromatic rings would bind to the enzyme by hydrophobic interactions (Fig. **3**), the carboxylic and keto groups would interact by hydrogen bonding, and the SO_2 would bind by dipolar interactions. Shen *et al.* [4, 50] have proposed, along with the cooperative drug–enzyme-DNA-binding model, that substituent on N-1, C-2, and C-8 make hydrophobic interactions with another molecule of AMFQ. Binding to the DNA strand is suggested to involve a hydrogen-bonding domain on the drug, comprising the C-3 carboxyl, the keto at C-4, and the C-6 fluorine. Furthermore, Shen postulated that bulky substituents are tolerated and that the substituent at C-7 is involved in drug–enzyme interactions through electrostatic forces [4, 50]. These conclusions were also confirmed by SAR studies reported by other researchers [39, 44].

The pharmacophore model presented herein and the accepted model from Shen [4, 50], agree in two important conclusions: (i) HBA and HYD interactions on FQ moiety, and (ii) the three functional domains on the quinolone molecule, defining C7 as the only position where the substitution with bulky groups are tolerated. The addition of various functional groups may increase interactions with the enzyme. The pharmacophore model presented herein shows two additional interactions for the dual targeting fluoroquinolones (BSFQs and BCFQs), HBA on the SO_2 group and HYD on the BS' or BC's phenyl rings.

CONCLUSIONS

A series of AMFQs, including the BSFQs and BCFQs, with anti Sa activity was studied in order to understand the structural requirements for this "dual targeting" property. Molecular modeling and 3D-QSAR studies were performed to explain the enhanced antibacterial *in vitro* activity when compared with NOR and CIP. In particular, disclosing the actual involvement of SO_2 and phenyl group in the interaction with the receptor.

The conformational analysis confirms that several conformations could be responsible for the activity of these molecules. The ax form has four conformers with minimum energy; which could be interchangeable ($\Delta E = 2.5$ kcal/mol). The eq form has only one global minimum and several conformations as local minima with $E < 2$ kcal/mol.

On the basis of QSAR analysis of this congeneric series of BSFQs, using both empirical and theoretical descriptors of the substituent of the molecular structure, it could be concluded that the electronic distribution of the BS group, modulated by the *p*-substituents, is the determining factor connected with inhibitory potency.

From the results obtained from 3D-QSAR and pharmacophore generation (Catalyst) the following conclusions can be drawn:

- It agrees with previous hypothesis from other authors that followed different methodologies.

- It agrees with observations from SAR analyses and results from QSAR studies.

- It shows that the interactions of the substituent at the N-7d are relevant for binding to the target enzyme.

- QSAR results show that small electron donor substituents will be optimum for biological activity.

- The proposed pharmacophore shows that the phenyl (BS group) is necessary for enzyme interaction. The substituents on this ring that increase the accepting capacity of the BS would increase the affinity toward the target enzyme.

- The proposed pharmacophore shows that the SO_2 group is involved in the interaction with the biological target through HBA, and the 3D QSAR demonstrated that electronic distribution on SO is an important descriptor of the interaction.

- 3D QSAR results show that the biological activity correlates with the size of the substituent and LUMO, meaning that there are charge transference interactions with the target enzyme.

- The presence of two aromatic systems (FQ + BS) in the pharmacophore reinforces the theories about the formation of a charge transfer complex (CTC) within fluoroquinolones and its target enzyme.

We postulate that the enhanced potency of BSFQs against Sa strains compared to parent compounds CIP and NOR could be caused by the presence of a BS substituent on the piperazinyl of C-7 that result in enhanced binding to DNA gyrase of Sa, although their greater ability to enter

bacterial cells by diffusion and a reduced susceptibility to FQ-specific efflux pumps could also make a contribution.

ACKNOWLEDGEMENTS

REFERENCES

[1]　Pan, X.-S.; Hamlyn, P.J.; Talens-Visconti, R.; Alovero, F.L.; Manzo, R.H.; Fisher, L.M. Small-colony mutants of *Staphylococcus aureus* allow selection of *gyrase*-mediated resistance to dual-target fluoroquinolones. *Antimicrob. Agents Chemother.,* **2002**, *46*(8), 2498-2506.

[2]　Strahilevitz, J.; Hooper, D.C. Dual targeting of topoisomerase IV and gyrase to reduce mutant selection: Direct testing of the paradigm by using wck-1734, a new fluoroquinolone, and ciprofloxacin. *Antimicrob. Agents Chemother.,* **2005**, *49*(5), 1949-1956.

[3]　Hooper, D.; Rubinstein, E. *Quinolone antimicrobial agents, 3rd edition,* **2002**.

[4]　Shen, L.L.; Mitscher, L.A.; Sharma, P.N.; O'Donnell, T.J.; Chu, D.T.W.; Cooper, C.S.; Rossen, T.; Pernet, A.G. Mechanism of inhibition of DNA gyrase by quinolone antibacterials: A cooperative drug-DNA binding model. *Biochemistry,* **1989**, *28*, 3886-3894.

[5]　Allemandi, D.A.; Alovero, F.L.; Manzo, R.H. In-vitro activity of new sulfanilyl fluoroquinolones against *Staphylococcus aureus*. *J. Antimicrob. Chemother.,* **1994**, *34*(2), 261-265.

[6]　Manzo, R.H.; Allemandi, D.A.; Perez, J.D. Antibacterial 7-[4-[(4-aminophenyl)sulfonyl]-1-piperazinyl]-6-fluoro-1,4-dihydro-4-oxoquinoline-3-carboxylic acid derivatives and synthesis thereof. US5395936, 1995.

[7]　Alovero, F.; Nieto, M.; Mazzieri, M.R.; Then, R.; Manzo, R.H. Mode of action of sulfanilyl fluoroquinolones. *Antimicrob. Agents Chemother.,* **1998**, *42*(6), 1495-1498.

[8]　Nieto, M.J.; Alovero, F.L.; Manzo, R.H.; Mazzieri, M.R. A new class of fluoroquinolones: Benzenesulfonamidefluoroquinolones (BSFQs), antibacterial activity and SAR studies. *Eur. J. Med. Chem.,* **1999**, *34*(3), 209-214.

[9]　Nieto, M.J.; Alovero, F.L.; Manzo, R.H.; Mazzieri, M.R. Benzenesulfonamide analogs of fluoroquinolones. Antibacterial activity and QSAR studies. *Eur. J. Med. Chem.,* **2005**, *40*(4), 361-369.

[10]　Alovero, F.; Barnes, A.; Nieto, M.; Mazzieri, M.R.; Manzo, R.H. Comparative study of new benzenesulphonamide fluoroquinolones structurally related to ciprofloxacin against selected ciprofloxacin-susceptible and -resistant Gram-positive cocci. *J. Antimicrob. Chemother.,* **2001**, *48*(5), 709-712.

[11]　Alovero, F.L.; Pan, X.-S.; Morris, J.E.; Manzo, R.H.; Fisher, L.M. Engineering the specificity of antibacterial fluoroquinolones: Benzenesulfonamide modifications at c-7 of ciprofloxacin change its primary target in *Streptococcus pneumoniae* from topoisomerase IV to gyrase. *Antimicrob. Agents Chemother.,* **2000**, *44*(2), 320-325.

[12]　Nieto, M.J.; Alovero, F.L.; Manzo, R.H.; Mazzieri, M.R. Benzene-carboxamide analogs of fluoroquinolones (BCFQs). Antibacterial activity and sar studies. *Lett. Drug Des. Discov.,* **2006**, *3*(2), 108-111.

[13]　Accelrys *Catalyst*, 48; Accelrys: Burlington, MA.

[14]　Schaftenaar, G.; Noordik, J.H. Molden: A pre- and post-processing program for molecular and electronic structures. *J. Comp.Aided Mol. Des.,* **2000**, *14*(2), 123-134.

[15]　Dewar, M.J.S.; Zoebisch, E.G.; Healy, E.F.; Stewart, J.J.P. Development and use of quantum mechanical molecular models. 76. Am1: A new general purpose quantum mechanical molecular model. *J. Am. Chem. Soc.,* **1985**, *107*(13), 3902-3909.

[16]　Semichem, I. *Ampac 8*, AMPAC 8; Semichem, Inc.: Shawnee, KS 66222., 1992-2004.

[17]　Stewart, J.P.P. *Winmopac*, Fujitsu Limited: Tokyo, Japan, 1997.

[18]　StatSoft *Statistica*, 4.1; StatSoft: Tulsa, OK, 2005.

[19]　Gund, P. Three-dimensional pharmacophoric pattern searching. *Prog. Mol. Subcell. Biol.,* **1977**, *5*, 117-143.

[20]　Brooks, B.R.; Bruccoleri, R.E.; Olafson, B.D.; States, D.J.; Swaminathan, S.; Karplus, M. Charmm: A program for macromolecular energy, minimization, and dynamics calculations. *J. Comp. Chem.,* **1983**, *4*(2), 187-217.

[21]　Smellie, A.; Teig, S.L.; Towbin, P. Poling: Promoting conformational variation. *J. Comp. Chem.,* **1995**, *16*(2), 171-187.

[22]　R.A.Fisher. *The design of experiments*. 9th ed. Hafner Publishing Company: New York, NY, **1971**.

[23]　De Benedetti, P.G.; Iarossi, D.; Folli, U.; Frassineti, C.; Menziani, C.; Cennamo, C. Quantitative structure activity relationships in dihydropteroate synthase inhibition by multisubstituted sulfones. Design and synthesis of some new derivatives with improved potency. *J. Med. Chem.,* **1989**, *32*, 2396-2399.

[24]　De Benedetti, P.G.; Iarossi, D.; Menziani, C.; Caiolfa, V.; Frassineti, C.; Cennamo, C. Quantitative structure-activity analysis in dihydropteroate synthase inhibition by sulfones. Comparison with sulfanilamides. *J. Med. Chem.,* **1987**, *30*, 459-464.

[25]　De Benedetti, P.G. Molecular modeling and quantitative structure-activity analysis of antibacterial sulfanilamides and sulfones. *Prog. Drug Res.,* **1991**, *36*, 361-417.

[26]　Ohta, M.; Koga, H. Three dimensional structure-activity relationships and receptor mapping of n1-substituents of quinolone antibacterials. *J. Med. Chem.,* **1991**, *34*, 131-139.

[27]　Chung, S.K.; Sun, J.H. Geometry mapping of n(1)-substituents of quinolone antibacterials and the antibacterials mode of actions. *Korean J. Med. Chem.,* **1993**, *3*, 148-161.

[28]　Turel, I.; Leban, I.; Klintschar, G.; Bukovec, N.; Zalar, S. Synthesis, crystal structure, and characterization of two metal-quinolone compounds. *J. Inorg. Biochem.,* **1997**.

[29]　Menziani, M.C.; Cocchi, M.; De Benedetti, P.G. A molecular dynamics simulation of sequence-directed recognition peptides interacting with bigendothelin. *J. Mol. Struct.,* **1993**, *286*, 95-108.

[30]　Liang, G.; Bays, J.P.; Bowen, J.P. Ab initio calculations and molecular mechanics (mm#) force field development for sulfonamide and its alkyl derivatives. *J. Mol. Struct.,* **1997**, *401*, 165-179.

[31]　Nieto, M.J.; Alovero, F.L.; Manzo, R.H.; Mazzieri, M.R. A new clas of fluoroquinolones: Benzenesulfonamidefluoroquinolones (BSFQs). Antibacterial activity and sar studies. *Eur. J. Med. Chem.,* **1999**, *34*(3), 209-214.

[32]　Reuman, M.; Daum, S.J.; Singh, B.; Wentland, M.P.; Perni, R.B.; Pennock, P.; Carabateas, P.M.; Gruett, M.D.; Saindane, M.T.; et al. Synthesis and antibacterial activity of some novel 1-substituted 1,4-dihydro-4-oxo-7-pyridinyl-3-quinolinecarboxylic acids. Potent antistaphylococcal agents. *J. Med. Chem.,* **1995**, *38*(14), 2531-2540.

[33]　Gordeev, M.F.; Hackbarth, C.; Barbachyn, M.R.; Banitt, L.S.; Gage, J.R.; Luehr, G.W.; Gomez, M.; Trias, J.; Morin, S.E.; Zurenko, G.E.; Parker, C.N.; Evans, J.M.; White, R.J.; Patel, D.V. Novel oxazolidinone-quinolone hybrid antimicrobials. *Bioorg. Med. Chem. Lett.,* **2003**, *13*(23), 4213-4216.

[34]　Hubschwerlen, C.; Specklin, J.-L.; Sigwalt, C.; Schroeder, S.; Locher, H.H. Design, synthesis and biological evaluation of oxazolidinone-quinolone hybrids. *Bioorg. Med. Chem.,* **2003**, *11*(10), 2313-2319.

[35]　Butler, M.M.; LaMarr, W.A.; Foster, K.A.; Barnes, M.H.; Skow, D.J.; Lyden, P.T.; Kustigian, L.M.; Zhi, C.; Brown, N.C.; Wright, G.E.; Bowlin, T.L. Antibacterial activity and mechanism of action of a novel anilinouracil-fluoroquinolone hybrid compound. *Antimicrob. Agents Chemother.,* **2007**, *51*(1), 119-127.

[36]　Robertson, G.T.; Bonventre, E.J.; Doyle, T.B.; Du, Q.; Duncan, L.; Morris, T.W.; Roche, E.D.; Yan, D.; Lynch, A.S. In vitro evaluation of cbr-2092, a novel rifamycin-quinolone hybrid antibiotic: Studies of the mode of action in *Staphylococcus aureus*. *Antimicrob. Agents Chemother.,* **2008**, *52*(7), 2313-2323.

[37]　Bhanot, S.K.; Singh, M.; Chatterjee, N.R. The chemical and biological aspects of fluoroquinolones reality and dreams. *Curr. Pharm. Des.,* **2001**, *7*(5), 311.

[38]　Foroumadi, A.; Mansouri, S.; Kiani, Z.; Rahmani, A. Synthesis and in vitro antibacterial evaluation of n-[5-(5-nitro-2-thienyl)-1,3,4-thiadiazole-2-yl] piperazinyl quinolones. *Eur. J. Med. Chem.,* **2003**, *38*(9), 851-854.

[39]　Llorente, B.; Leclerc, F.; Cedergren, R. Using sar and qsar analysis to model the activity and structure of the quinolone--DNA complex. *Bioorg. Med. Chem.,* **1996**, *4*(1), 61-71.

[40]　Domagala, J.M. Structure-activity and structure-side-effect relationships for the quinolone antibacterials. *J. Antimicrob. Chemother.,* **1994**, *33*(4), 685-706.

[41]　Koga, H.; Itoh, A.; Murayama, S.; Suzue, S.; Irikura, T. Structure-activity relationships of antibacterial 6,7- and 7,8-disubstituted 1-

alkyl-1,4-dihydro-4-oxoquinoline-3-carboxylic acids. *J. Med. Chem.,* **1980**, *23*(12), 1358-1363.

[42]   Emami, S.; Shafiee, A.; Foroumadi, A. Structural features of new quinolones and relationship to antibacterial activity against Gram-positive bacteria. *Mini Rev. Med. Chem.,* **2006**, *6*(4), 375-386.

[43]   Foroumadi, A.; Emami, S.; Mehni, M.; Moshafi, M.H.; Shafiee, A. Synthesis and antibacterial activity of n-[2-(5-bromothiophen-2-yl)-2-oxoethyl] and n-[(2-5-bromothiophen-2-yl)-2-oximinoethyl]derivatives of piperazinyl quinolones. *Bioorg. Med. Chem. Lett.,* **2005**, *15*(20), 4536-4539.

[44]   Mitscher, L.A. Bacterial topoisomerase inhibitors: quinolone and pyridone antibacterial agents. *Chem. Rev.,* **2005**, *105*(2), 559-592.

[45]   Van Bambeke, F.; Michot, J.M.; Van Eldere, J.; Tulkens, P.M. Quinolones in 2005: An update. *Clin. Micr. Infect.,* **2005**, *11*(4), 256-280.

[46]   Peterson, L.R. Quinolone molecular structure-activity relationships: What we have learned about improving antimicrobial activity. *Clin. Infect. Dis.,* **2001**, *33 Suppl 3*, S180-186.

[47]   Kerns, R.J.; Rybak, M.J.; Kaatz, G.W.; Vaka, F.; Cha, R.; Grucz, R.G.; Diwadkar, V.U. Structural features of piperazinyl-linked ciprofloxacin dimers required for activity against drug-resistant strains of *Staphylococcus aureus. Bioorg. Med. Chem. Lett.,* **2003**, *13*(13), 2109-2112.

[48]   Kerns, R.J.; Rybak, M.J.; Kaatz, G.W.; Vaka, F.; Cha, R.; Grucz, R.G.; Diwadkar, V.U.; Ward, T.D. Piperazinyl-linked fluoroquinolone dimers possessing potent antibacterial activity against drug-resistant strains of *Staphylococcus aureus. Bioorg. Med. Chem. Lett.,* **2003**, *13*(10), 1745-1749.

[49]   Hooper, D.C. Mechanisms of action of antimicrobials: Focus on fluoroquinolones. *Clin. Infect. Dis.,* **2001**, *32*, S9.

[50]   Morrissey, I.; Hoshino, K.; Sato, K.; Yoshida, A.; Hayakawa, I.; Bures, M.G.; Shen, L.L. Mechanism of differential activities of ofloxacin enantiomers. *Antimicrob. Agents Chemother.,* **1996**, *40*(8), 1775-1784.

[51]   Piddock, L.J.V.; Jin, Y.F.; Griggs, D.J. Effect of hydrophobicity and molecular mass on the accumulation of fluoroquinolones by *Staphylococcus aureus. J. Antimicrob. Chemother.,* **2001**, *47*(3), 261-270.

[52]   Beyer, R.; Pestova, E.; Millichap, J.J.; Stosor, V.; Noskin, G.A.; Peterson, L.R. A convenient assay for estimating the possible involvement of efflux of fluoroquinolones by *Streptococcus pneumoniae* and *Staphylococcus aureus*: Evidence for diminished moxifloxacin, sparfloxacin, and trovafloxacin efflux. *Antimicrob. Agents Chemother.,* **2000**, *44*(3), 798-801.